Computational Studies of (HIO_3) Isomers and the HO_2 + IO Reaction Pathways

Evangelos Drougas and Agnie M. Kosmas*

Department of Chemistry, University of Ioannina, Ioannina 45110, Greece

Received: December 21, 2004; In Final Form: March 8, 2005

The geometries, harmonic vibrational frequencies, relative energetics, and enthalpies of formation of (HIO_3) isomers have been examined using quantum mechanical methods. At all levels of theory employed, MP2, B3LYP, and CCSD(T), the lowest energy structure is found to be the $HOIO_2$ form, which shows particular stability. The two isomers HOOOI and HOOIO are closely located at the CCSD(T) level of theory. The higher energy structure is HIO_3. The interisomerization transition states have been determined, along with the transition states involved in the various pathways of the reaction HO_2 + IO.

1. Introduction

New observations of elevated concentrations of iodinated methanes in seawater and marine air samples have been reported recently by a number of workers.[1−4] As a result, the reactivity of IO radical acquires fresh interest owing to its long known role as an intermediate species in the tropospheric oxidation of iodine-containing compounds. Among its major loss processes the reaction with HO_2[5−9]

$$IO + HO_2 \rightarrow HOI + O_2 \quad (1)$$

plays an important role and leads to the formation of HOI, an assumed iodine sink compound in the atmosphere.

Due to its significance, the kinetics of reaction 1 have been examined several times, and large rate constants have been determined in all cases. In the older reports, Jenkin et al.[5] used the molecular modulation technique to measure the rate coefficient of reaction 1 as $k = 6.4 \times 10^{-11}$ cm^3 molecule^{-1} s^{-1} at 289 K and 760 Torr. Maguin et al.[6] employed a low-pressure discharge-flow/mass spectrometry technique to obtain $k = 10.3 \times 10^{-11}$ cm^3 molecule^{-1} s^{-1} at the same temperature. More recently, the rate coefficient was found to be $k = 7.1 \times 10^{-11}$ cm^3 molecule^{-1} s^{-1} at 298 K in the study of Canosa-Mas et al.,[7] while the temperature dependence was investigated by Cronkhite et al.[8] in the range 274−373 K, in N_2 buffer gas and at pressures of 12 and 25 Torr, and by Knight et al.[9] in the range rate 273−353 K and total pressures of 1.0−2.0 Torr He. The Arrhenius expressions resulting from the latter two studies

$$k = (9.3 \pm 3.3) \times 10^{-12} \exp(680 \pm 110/T) \text{ cm}^3 \text{ molecule}^{-1} \text{ s}^{-1} \quad (2)$$

and

$$k = (2.2 \pm 0.6) \times 10^{-11} \exp(400 \pm 80/T) \text{ cm}^3 \text{ molecule}^{-1} \text{ s}^{-1} \quad (3)$$

respectively, lead to values of the rate coefficient at room temperature in the same range as the former studies. Most importantly, however, they both predict slightly negative activation energies. The finding of a negative activation energy argues in favor of a long-range interaction between IO$^\bullet$ and HOO$^\bullet$ and a reaction mechanism through IO initial attack on the radical site in HOO$^\bullet$ to form a bound intermediate. The analogous ClO + HO_2 and BrO + HO_2 reactions[10−13] have both been shown to involve the formation of bound ($HClO_3$)[14] and ($HBrO_3$)[15,16] isomeric forms which through cyclic-type transition state configurations proceed to various production pathways. Hence, as pointed out by Cronkhite et al.,[8] a quantum mechanical study of (HIO_3) isomers is desirable and could significantly contribute to the understanding of the mechanism of reaction 1.

In the present work we perform a theoretical investigation of the isomeric forms of (HIO_3) species and the pathways of IO + HO_2 reaction. Geometries, harmonic vibrational frequencies, relative energetics, and enthalpies of formation of the main stationary points on the potential energy surface are determined using high-level quantum mechanical techniques. The results are discussed in relation to the available experimental evidence, and an interesting comparison is carried out with the analogous Cl and Br systems.

2. Computational Methods

The starting point of our work has been to select a suitable and effective method for the treatment of the present system, which contains the heavy iodine atom. Density functional theory (at the level of Becke three-parameter hybrid functional B3LYP)[17] and Møller−Plessett second-order correlation energy correction method (MP2)[18] are employed to perform the geometry optimizations. Further refinement of the energetics is accomplished by conducting single-point energy calculations at the CCSD(T) level of theory.

The selection of the appropriate basis set is also crucial for the accuracy of the calculations. Indeed, inclusion of polarization functions has been shown to be very important for the proper description of iodine polyoxides.[19,20] Recently, in the study of the related (HIO) and (HIO_2) systems, Begovic et al.[21] have made a detailed examination of the performance of several basis sets in the description of test species containing similar kinds of bonds. Following their analysis we have combined the present methodologies with similar basis sets. More specifically, the double-ζ valence basis set augmented with p and d diffuse and polarization functions, hereafter called LANL2DZdp, is used for oxygen.[22] The double-ζ valence basis set combined with

* Author to whom correspondence should be addressed. E-mail: amylona@cc.uoi.gr.

10.1021/jp044197j CCC: $30.25
Published on Web 04/09/2005

TABLE 1: Electronic Energies Including ZPE Corrections (hartrees) and Reaction Enthalpies (kcal mol^{-1}) for the System HO_2 + IO[a]

species	B3LYP	MP2	CCSD(T)	ΔE	ΔH_r^{298}	ZPE
HOOOI	−237.504 553	−236.839 316	−236.892 192	−11.1	−9.8	12.3
HOOIO	−237.507 068	−236.849 498	−236.892 360	−11.2	−9.9	12.0
$HOIO_2$	−237.568 637	−236.812 902	−236.955 819	−51.0	−50.1	11.9
HIO_3	−237.457 924	−236.812 902	−236.844 566	18.7	19.6	10.8
TS1	−237.463 532	−236.817 837	−236.861 731	8.0	8.9	11.9
TS2	−237.467 644	−236.819 092	−236.870 337	2.6	1.8	9.8
TS3	−237.416 808	−236.768 606	−236.801 999	45.4	43.0	8.8
TS4	−237.451 889	−236.821 709	−236.868 102	4.0	1.5	8.4
TS5	−237.493 419	−236.844 830	−236.871 289	2.0	0.1	9.4
TS6	−237.449 850	−236.809 672	−236.832 619	26.2	24.3	9.2
HO_2 + IO	−237.489 212	−236.794 469	−236.874 422[b]	0.0	0.0	10.1
HOI + $O_2(^1\Delta)$	−237.493 971	−236.853 949	−236.911 219[c]	−23.1	−21.7	9.7
HOI + $O_2(^3\Sigma)$	−237.555 471	−236.902 043	−236.946 903	−45.5	−42.3	10.0
HI + O_3	−237.453 392	−236.811 934	−236.847 391	15.3	14.4	9.6
HO + OIO	−237.545 781	−236.827 810	−236.877 884	−2.2	−1.8	8.0

[a] The basis sets employed are LANL2DZdp for oxygen, LANL2DZspdf+ECP for iodine, and 6-311++G(3df, 3dp) for hydrogen. [b] The IO electronic energy includes a spin−orbit splitting value of 2 kcal mol^{-1}.[19] [c] The energy of $O_2(^1\Delta)$ is calculated using complex orbitals at the RMP2/LANL2DZdp level.

the relativistic effective core potential of Wadt and Hay[23] and augmented with uncontracted s and p diffuse functions (exponents 0.0569 and 0.0330, respectively) and d and f polarization functions (exponents 0.292 and 0.441, respectively),[24] hereafter called LANL2DZspdf+ECP, is used for iodine. The 6-311++G-(3df,3pd) basis set is used for hydrogen.

The study of the singlet surface requires the calculation of the oxygen molecule in the $^1\Delta_g$ state.[10] The energy calculations that include the standard basis sets repeatedly fail to predict the correct experimental energy spacing between singlet and triplet oxygen, 22.5 kcal mol^{-1}, and they usually predict a much higher value around 30 kcal mol^{-1}.[11,14−16] To achieve this purpose, we must use complex orbitals. We have thus calculated the energy of the $^1\Delta_g$ state of the O_2 molecule using complex orbitals at the RMP2/LANL2DZpd level, and we have succeeded in producing a theoretical spacing value of 22.4 kcal mol^{-1}, in excellent agreement with the experimental result.

Vibrational frequency analysis was performed at both methods of optimization to identify the structures obtained as real minima or saddle points. The transition states were characterized by one imaginary frequency as first-order saddle points, and they were further confirmed by connecting the related reactants and products by intrinsic reaction coordinate (IRC)[25] analysis. All quantum mechanical calculations were performed with the Gaussian 98 A.9 program package.[26]

3. Results

Ten structures have been investigated in total: four energy minima and six transition states for isomerization and production pathways. The HO + OIO channel has also been computed. Calculated structural and harmonic frequency results are consistent at both MP2 and B3LYP levels. The optimized structures for all stationary points examined along with the geometric parameters at the MP2 level are presented in Figure 1. The electronic energies and the relative stabilities at the MP2, B3LYP, and CCSD(T) levels are collected in Table 1. Table 2 summarizes the calculated harmonic frequencies at the MP2 level, and Table 3 displays the calculated heats of formation including a comparison with literature data for the corresponding Cl and Br derivatives. Finally, the energy profile of the reaction with respect to the most stable isomer, based on the CCSD(T) results, is depicted in Figure 2.

Energy Minima. Among the most important features of the potential energy surface of reaction 1 are the two nascent

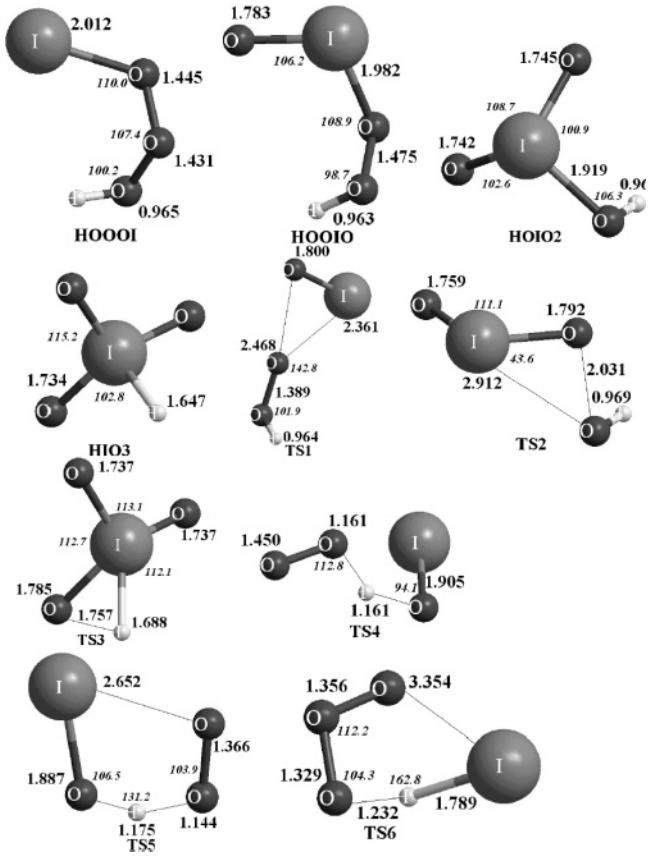

Figure 1. Structures of the most important stationary points on the potential energy surface of the reaction HO_2 + IO at the MP2 level (basis set described in text).

association energy minima, HOOOI and HOOIO. The first structure is formed when the two reactants, HO_2 and IO radicals, approach each other with their oxygen atom ends. The equilibrium ground state presents a skew geometry and resembles the HOOOCl and HOOOBr structures, while the values of the geometric parameters are close to the corresponding values in the HOOI system.[21] The dihedral angles HOOO and OOOI are found to be −92.6° and 82.7°, respectively. The HO−O and O−OI bond lengths, 1.431 and 1.445 Å, are slightly longer than the O−O distance, 1.428 Å, in HOOI and the O−I bond distance, 2.012 Å, is slightly shorter than that in HOOI, 2.058 Å.[21] The HOO angle (100.2°) is smaller than the OOI angle

TABLE 2: Unscaled Vibrational Harmonic Frequencies of Stationary Points Involved in the Reaction HO_2 + IO at the MP2 Level of Theory[a]

species	frequencies (cm^{-1})
HOOOI	112, 258, 386, 505, 573, 695, 879, 1397, 3797
HOOIO	99, 222, 273, 336, 528, 824, 923, 1352, 3840
$HOIO_2$	84, 269, 306, 329, 602, 951, 971, 988, 3789
TS1	179i, 144, 179, 433, 526, 915, 974, 1376, 3783
TS2	606i, 115,131, 194, 299, 661, 682, 955, 3788
TS3	1557i, 262, 284, 314, 422, 941, 977, 1002, 1987
TS4	2149i, 60, 148, 270, 633, 738, 910, 1342, 1789
TS5	923i, 191, 244, 418, 532, 750, 1186, 1380, 1854
TS6	962i, 90, 236, 437, 585, 717, 1077, 1096, 2211

[a] The basis sets employed are LANL2DZdp for oxygen, LANL2DZspdf+ECP for iodine, and 6-311++G(3df, 3dp) for hydrogen.

TABLE 3: Calculated Dissociation Energies, D_0, and Enthalpies of Formation, ΔH_f^0 (kcal mol^{-1}), for (HIO_3) Isomers Based on the CCSD(T) Energetics and Comparison with ($HClO_3$) and ($HBrO_3$)[a]

	I						
	HO_2 + IO			OH + OIO		Cl[e]	Br[f]
	D_0	ΔH_f^0	ΔH_f^{298}	D_0	ΔH_f^0	ΔH_f^0	ΔH_f^0
HOOOX	9.8	24.2[b] 21.9[c]	19.4[d]	−8.9	19.5	9.1	13.6
HOOXO	9.9	24.1[b] 21.6[c]	19.3[d]	−8.8	19.4	25.3	26.2
$HOXO_2$	51.2	−15.2[b] −17.8[c]	−20.1[d]	−48.8	−20.4	4.2	5.7
HXO_3	−19.3	53.3[b] 51.0[c]	48.4[d]	20.9	49.3	46.1	71.6

[a] X = I, Cl, or Br. [b] ΔH_f^0(IO) (kcal mol^{-1}) = 30.7.[18] [c] ΔH_f^0(IO) (kcal mol^{-1}) = 28.1.[32] [d] ΔH_f^{298}(IO) (kcal mol^{-1}) = 26.7,[33] ΔH_f^0(OIO) (kcal mol^{-1}) = 19.2.[18] [e] Reference 13. [f] Reference 14.

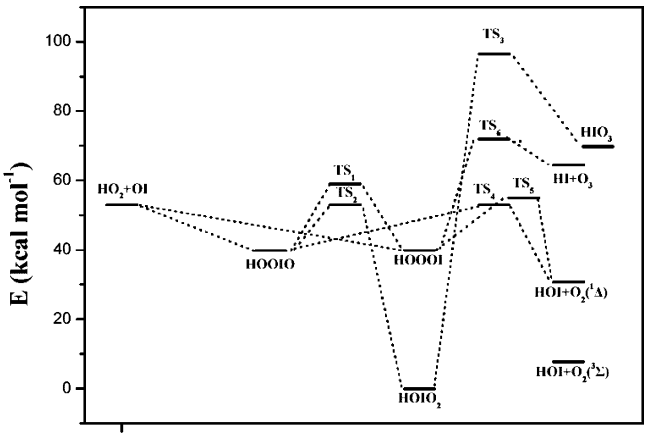

Figure 2. Relative energy profile with respect to the most stable isomer $HOIO_2$ at the CCSD(T) level of theory (basis set described in text).

(110.0°) due to the large amount of repulsion between the lone pairs of electrons of iodine with those of oxygen.

The other association minimum that can be formed is HOOIO. This, too, is a skewed structure with oxygen as the terminal atom. The dihedral angle HOOI is 101.2° while the angle OOIO is −79.1°. The bond angle OIO, 106.2°, is a little narrower that the OOI angle, 108.9°, due to the greater degree of repulsion between the lone pairs of electrons on iodine with those on the oxygen atom. The bond distances O−I and I−O are found quite different, 1.982 and 1.783 Å respectively, in agreement with the respective 1.989 and 1.812 Å in HOIO.[21] They thus reflect the considerable shrinkage of the bond distance due to the hypervalent character between iodine and the terminal oxygen atom as compared to the normal-valent bonding in HOOOI, where O−I = 2.012 Å. An interesting feature regarding the two association minima is their comparable stability. HOOIO is comparable to HOOOI, being lower in energy by 6.4 kcal mol^{-1} at the MP2 level and 1.6 kcal mol^{-1} at the B3LYP level, as is readily deduced from Table 1. At the CCSD(T) level HOOIO is found to be similar to HOOOI, with only a 0.1 kcal mol^{-1} difference. Consequently, each of the two isomers presents a similar probability to be formed as an intermediate complex in the HO_2 + IO reaction. Similar stability trends between the same type of isomers have been observed in other related iodine oxides such as HOOI, HOIO[21] and CH_3OOI, CH_3OIO,[27] where the XOIO forms are even found to be more stable than XOOI. This tendency is entirely different from what has been observed in the ($HClO_3$) and ($HBrO_3$) families.[14−16] The corresponding HOOOCl and HOOOBr adducts have been found to be substantially more stable than HOOClO and HOOBrO, and they are preferably formed as intermediates in the HO_2 + XO reactions.

The third isomeric form is iodic acid, $HOIO_2$, a stable white solid at room temperature, usually obtained by oxidizing iodine with concentrated nitric acid or hydrogen peroxide.[28] Here, the multiple bond characteristics between iodine and the terminal oxygen atoms are enhanced and the I−O bond distances, 1.745 (1.742) Å, are much shorter than the O−I bond distance, 1.919 Å. The interesting feature is its striking stability compared to the other isomeric forms. $HOIO_2$ is predicted to be lower in energy than HOOOI by 47.6 and 38.6 kcal mol^{-1} in the MP2 and B3LYP calculations, respectively, and by 41.4 kcal mol^{-1} at the CCSD(T) level. This is quite different from what is observed in the ($HClO_3$) and ($HBrO_3$) families, where the $HOXO_2$ forms have been found to be just a few kilocalories per mole lower than HOOOX, with the difference depending on the level of theory employed.[14−16] The high stability of $HOIO_2$ is also contrary to the stability order of the HIO_2 species, which is the least stable isomer in the (HIO_2) family. The different behavior is easily explained if we consider the natural charges on the hypervalent I and the H and HO partners. In HIO_2[21] the large positive charge on I forces H to be charged negatively and destabilizes HIO_2, while in the case of the iodic acid, $HOIO_2$, the highly electropositively charged iodine combines with the strongly electronegative HO moiety and produces the high stabilization of this compound.

The final isomer is HIO_3 with the three oxygen atoms forming the base of the pyramid. The I−O bond distance (1.734 Å) is the shortest among all other terminal I−O bonds, resulting from the I═O multiple bonding characteristics in HIO_3. Such an effect does not occur in normal-valent HOOOI and appears only for the terminal oxygen atoms in HOOIO and $HOIO_2$. HIO_3 is the most unstable isomer, located around 70 kcal mol^{-1} higher than $HOIO_2$ at all levels of theory employed.

The examination of the atomic charges is, indeed, profitable for interpreting the high stability of the HOOIO and $HOIO_2$ forms, the high instability of HIO_3, and their differences compared with the ($HClO_3$) and ($HBrO_3$) families. As already mentioned, the stabilization of the various forms appears to correlate strongly with the increasing polarization acquired in I−O bonding. In normal-valent HOOOI, the Mulliken charges are found to be −0.192 on O and +0.162 on I, indicating a mild polarization of the O−I bond. In the hypervalent isomers, however, the corresponding charges increase dramatically and we obtain −0.253 on bridged O, 0.719 on I, and −0.512 on terminal O for HOO−I−O and −0.502 on bridged O, 1.151 on I, and −0.495 on terminal O for HO−I−O_2. Thus, the strong ionic character of the I−O bonding in HOOIO and $HOIO_2$

combined with an electronegative fragment like HOO or HO contributes significantly to the high stabilization of these isomeric forms. Significant polarization of the halogen−oxygen bond has also been observed in the Cl−O and Br−O[29] cases but not as strong as that observed in the iodine polyoxides. The much lower electronegativity of I allows the higher polarization of the I−O bonding and considerably stabilizes the hypervalent structures, HOOIO and $HOIO_2$. On the other hand, the same polarization leads to the high instability of HIO_3 because the highly positive charged I with an atomic charge of 1.436 forces a slight negative charge, −0.037, on H.

In summary, the structural characteristics of (HIO_3) isomers closely resemble those of the members of ($HClO_3$) and ($HBrO_3$) families. Substantial differences are observed in the relative energetics (Tables 1 and 3) that lead to the high stability of the $HOIO_2$ isomer and the similar stabilities of HOOOI and HOOIO, to be discussed in the following sections.

Isomerization Channels. The first isomerization pathway examined is the HOOIO ↔ HOOOI interconversion. The corresponding transition state TS1 (Figure 1) results from the migration of the iodine atom through the elongation of the O−I and I−O bond distances from 1.982 and 1.783 Å in HOOIO to 2.361 and 1.800 Å in TS1 and the synchronous decrease of the HO−O bond from 1.475 to 1.389 Å. The associated barrier is relatively high, located at 18.8 kcal mol^{-1} above HOOIO at the CCSD(T) level. The second isomerization transition state determined is TS2, for the HOOIO ↔ $HOIO_2$ interconversion, located at 11.6 kcal mol^{-1} above HOOIO at the CCSD(T) level. It results from the iodine approach to the HO part of HOOIO with a simultaneous decrease of the O−I bond distance from 1.982 to 1.792 Å and the considerable opening of the HO−O distance from 1.475 to 2.031 Å. The interisomerizations present relatively low barriers compared with the reactants HO_2 + IO. TS2 in particular, placed only 1.7 kcal mol^{-1} higher than HO_2 + IO, is quite comparable to the reactants, taking into account the uncertainty limits of the methodology. Therefore, it may be considered to represent a reaction pathway leading to the formation of $HOIO_2$ if stabilization conditions are favorable.

The final isomerization transition state determined, TS3, corresponds to the $HOIO_2$ ↔ HIO_3 process and results from the decrease of the O−I bond from 1.919 Å in $HOIO_2$ to 1.785 Å in TS3 and the increase of the H−O distance from 0.968 to 1.757 Å. The associated barrier is located very high, 93.1 kcal mol^{-1} with respect to $HOIO_2$ and 43.0 kcal mol^{-1} above the reactants, making this isomerization route highly improbable.

Production Pathways. It is clear from the similar stabilities of HOOOI and HOOIO at the CCSD(T) level that both structures are equally probable on energetic grounds, to be formed as nascent complexes in reaction 1. As already said, this is an interesting difference from the HO_2 + ClO, BrO reactions, where the HOOClO and HOOBrO adducts are found to be ∼15 kcal mol^{-1} higher than HOOOCl and HOOOBr at the CCSD(T) level[14−16] and their formation is thus much less probable. Once activated HOOIO and HOOOI are formed as HO_2 and IO approach each other, they may subsequently follow several production pathways. One has been already mentioned: the HOOIO ↔ $HOIO_2$ isomerization through the TS2 transition state, which leads to the very stable $HOIO_2$ product. This is an association rearrangement pathway, pressure dependent, that needs considerable stabilization of the product formed, but it is expected to gain in significance at elevated pressures where stabilization of the excess energy is feasible.

The other important reaction pathway is the channel leading to HOI + O_2 products. These products are obtained through either HOOOI or HOOIO formation and via TS4 and TS5 transition states, respectively. TS4 results from the migration of iodine atom in HOOOI, while TS5 is formed as the two ends of HOOIO approach and assume a ring geometry. The HOI + O_2 products are located at 20.9 kcal mol^{-1} in the singlet state and 42.3 kcal mol^{-1} in the triplet state below reactants at the CCSD(T) level, obtained through singlet−triplet coupling. TS5 is the lowest barrier determined in the potential energy surface of the reaction and represents the most probable pathway, located at the same energy level as the reactants HO_2 + IO. However, TS4 is comparable, located only 1.4 kcal mol^{-1} higher than TS5. Thus, the mechanism of HOI + $O_2(^1\Delta)$ production involves the intermediate formation of either of the two isomers, and really any route through either HOOIO or HOOOI will eventually lead to HOI + O_2. Both pathways are nearly equivalent and consistent with the large experimental rate coefficient measured for reaction 1, almost 1 order of magnitude larger than the rate coefficient of the HO_2 + ClO reaction.[11] This is another significant difference from the mechanism of HO_2 + ClO, BrO reactions where the HOX + O_2 production through the less stable HOOXO species presents a much lower energy barrier and comprises the preferable pathway while the barrier for HOX + O_2 production through HOOOX is considerably higher.

The system as already mentioned accesses the triplet state, HOI + $O_2(^3\Sigma)$, through spin−orbit coupling. All attempts, using both B3LYP and MP2 methods, to locate the HOOOI and HOOIO isomers on the triplet state and establish the triplet potential energy surface have failed.

The final pathway is endothermic and leads to HI + O_3 products through HOOOI intermediate formation and via the TS6 transition state. The geometry of TS6 results from the approach of the two ends of HOOOI to produce a cyclic structure like TS5. The associated barrier is very high, 24.3 kcal mol^{-1}, and the products HI + O_3 are higher located than the reactants by 14.4 kcal mol^{-1}, making this pathway quite unimportant.

4. Thermochemistry and Atmospheric Implications

To have a better picture of the relative stabilities of (HIO_3) isomers for atmospheric modeling and to present a more clear comparison with the ($HClO_3$) and ($HBrO_3$) species, the enthalpies of formation ΔH_f^0 and ΔH_f^{298} have been calculated and are depicted in Table 3. The calculations have been carried out considering the two dissociation pathways, namely to IO + HO_2 and HO + OIO decomposition products.

The main obstacle to the reliable calculation of ΔH_f for (HIO_3) isomers is the lack of accurate values for the heats of formation of IO and OIO. The uncertainty for the heat of formation of IO, in particular, is more than 15 kcal mol^{-1} in the range of theoretical and experimental evaluations reported in the literature. Misra et al.[19] in their study of the reaction of O atoms with CH_3I have made a theoretical calculation of the heat of formation of IO and a good coverage of the literature values as well. Indeed, estimates of ΔH_f(IO) are very widely scattered and range from 25.6 to 41.8 kcal mol^{-1}.[30] More recent calculations have produced values in the same region with a similar spreading.[21,31,32] Under these circumstances we have chosen to carry out the enthalpy of formation calculations for the most frequently quoted values: ΔH_f^0(IO) = 30.7 kcal mol^{-1},[19] 28.1 kcal mol^{-1},[33] and ΔH_f^{298}(IO) = 26.7 kcal mol^{-1} [34] for the IO + HO_2 dissociation route. For the other possible dissociation channel the calculated ΔH_f^0 value for OIO from Misra et al.,[19] 19.2 kcal mol^{-1}, has been employed. ΔH_f values

for HO and HO_2 have been taken from the literature.[36] The calculated heats of formation of (HIO_3) isomers with respect to both dissociation reactions, are summarized in Table 3. Fair agreement is observed between the values computed using the experimental estimates of Bedjanian et al.,[33,34] namely, 28.1 and 26.7 kcal mol^{-1} (117.8 and 111.7 kJ mol^{-1}) for ΔH_f^0 and ΔH_f^{298} of IO, respectively. Thus, they support the reliability of the experimental estimates for the heat of formation of IO and make the ΔH_f^0 values of ~30 kcal mol^{-1} appear rather too high.

The high stability of $HOIO_2$ isomer suggests the possibility for this compound to play a role in tropospheric chemistry. The ab initio calculations, summarized in Table 1 and Figure 2, indicate similar barriers for both the HOI + O_2 production channel and the isomerization pathways, particularly the HOOIO ↔ $HOIO_2$ isomerization. Therefore, $HOIO_2$ formation may be a possible reaction route under low-temperature and high-pressure conditions that facilitate stabilization of the product

$$HO_2 + IO \xrightarrow{M} HOOIO \rightarrow HOIO_2$$

and, consequently, iodic acid may act as a temporary reservoir species for iodine evolved in the marine boundary layer.

The last interesting feature in Table 3 is the comparison of (HIO_3) isomers with the ($HClO_3$) and ($HBrO_3$) species. In the Cl and Br series, the $HOXO_2$ structures too are the most stable adducts in their series but they are closely followed by the normal-valent isomers HOOOX. The hypervalent forms HOOXO are considerably more unstable. The iodine family shows significant differences. The $HOIO_2$ isomer is a very stable compound, by far much more stable than $HOClO_2$ and $HOBrO_2$, and it may thus be considered as a reservoir species for atmospheric I. Normal-valent HOOOI is more unstable than HOOOCl and HOOOBr, and it is located very near the hypervalent HOOIO. However, both are more stable than the HOOClO and HOOBrO structures. We attribute the differences in the stability of the (HIO_3) members compared to the ($HClO_3$) and ($HBrO_3$) isomers to the much lower electronegativity of I, which results in a better stabilization of the ionic I−O bonding in the HOOIO and $HOIO_2$ compounds.

5. Summary

The most important stationary points on the potential energy surface of the reaction HO_2 + IO have been characterized using ab initio and density functional theory methods. All structures were fully optimized at the MP2 and B3LYP levels of theory, and refinement of the energetics has been accomplished by performing single-point CCSD(T) calculations. Among the isomers of the (HIO_3) family, $HOIO_2$ is found to be particularly stable while HOOOI and HOOIO are relatively stable and comparable in energy. The last isomer, HIO_3, appears very unstable.

The mechanism of the reaction involves the initial formation of either HOOOI or HOOIO nascent intermediates. HOOIO via TS2 can isomerize to $HOIO_2$, which may be stabilized under favorable temperature and pressure conditions and make a temporary reservoir for iodine evolved in the marine boundary layer. The two adducts HOOOI and HOOIO may also proceed through transition states TS4 and TS5 respectively and lead to the reaction products, HOI + O_2. All routes are equivalent since the two minima are similar in energy and the corresponding energy barriers are found to be quite low, comparable in energy to those of the reactants. This is a substantial difference from the mechanism of the analogous HO_2 + ClO,[11] BrO[16] reactions which present high isomerization barriers to $HOClO_2$ and $HOBrO_2$ and hypervalent HOOClO and HOOBrO structures considerably higher located than HOOOCl and HOOOBr. Also in the Cl and Br systems, the energy barriers that lead to the products HOX + O_2 are much lower through intervening HOOXO rather than HOOOX formation, making the channels through HOOXO be the preferable reaction pathways in those cases.

Acknowledgment. The authors are deeply indebted to Prof. Paul Marshall for critical revision of the manuscript.

References and Notes

(1) Carpenter, L. J.; Sturges, W. T.; Penkett, S. A.; Liss, P. S.; Alicke, D.; Hebestreit, K.; Platt, U. *J. Geophys. Res*. **1999**, *104*, 1679.
(2) Vogt, R.; Sander, R.; von Glasow, R.; Crutzen, P. J. *J. Atmos. Chem*. **1999**, *32*, 375.
(3) O'Dowd, C. D.; Jimenez, J. L.; Bahreini, R.; Flagan, C. R.; Seinfeld, H. J.; Hameri, K.; Pirjola, L.; Kulmala, M.; Jennings, S. G.; Hoffmann, T. *Nature* **2002**, *417*, 632.
(4) Charles, E. K. *Nature* **2002**, *417*, 597.
(5) Jenkin, M. E.; Cox, R. A.; Hayman, G. D. *Chem. Phys. Lett*. **1991**, *177*, 272.
(6) Maguin, F.; Laverdet, G.; Le Bras, G.; Poulet, G. *J. Phys. Chem*. **1992**, *96*, 1775.
(7) Canosa-Mas, C. E.; Flugge, M. L.; Shah, D.; Vipond, A.; Wayne, R. P. *J. Atmos. Chem*. **1999**, *43*, 153.
(8) Cronkhite, J. M.; Stickel, R. E.; Nicovich, J. M.; Wine, P. H. *J. Phys. Chem. A* **1999**, *103*, 3228.
(9) Knight, G. P.; Crowley, J. N. *Phys. Chem. Chem. Phys*. **2001**, *3*, 393.
(10) Buttar, D.; Hirst, D. M. *J. Chem. Soc., Faraday Trans*. **1994**, *90*, 1811.
(11) Nickolaisen, S. L.; Roehl, C. M.; Blakeley, L. K.; Friedl, R. R.; Francisco, J. S.; Liu, R.; Sander, S. P. *J. Phys. Chem. A* **2000**, *104*, 308.
(12) Kaltsoyannis, N.; Rowley, D. M. *Phys. Chem. Chem. Phys*. **2002**, *4*, 419.
(13) Knight, G. P.; Beiderhase, T.; Helleis, F.; Moortgat, G. K.; Crowley, J. N. *J. Phys. Chem. A* **2000**, *104*, 1674.
(14) Francisco, J. S.; Sander, S. P. *J. Phys. Chem*. **1996**, *100*, 573.
(15) Guha, S.; Francisco, J. S. *J. Phys. Chem. A* **1998**, *102*, 2072.
(16) Guha, S.; Francisco, J. S. *J. Phys. Chem. A* **1999**, *103*, 8000.
(17) Becke, A. D. *J. Chem. Phys*. **1993**, *98*, 5648.
(18) Møller, C.; Plesset, M. S. *Phys. Rev*. **1934**, *46*, 618.
(19) Misra, A.; Berry, R. J.; Marshall, P. *J. Phys. Chem. A* **1997**, *101*, 7420.
(20) Papayannis, D.; Kosmas, A. M.; Melissas, V. S. *Chem. Phys. Lett*. **2001**, *349*, 299.
(21) Begovic, N.; Markovic, Z.; Anic, S.; Kolar-Anic, L. *J. Phys. Chem. A* **2004**, *108*, 651.
(22) (a) Dunning, T. H., Jr.; Hay, P. J. In *Methods of Electronic Structure, Theory*; Schaefer, H. F., III, Ed.; Plenum Press: New York, 1977; Vol. 2. (b) Basis sets obtained from the *Extensible Computational Chemistry Environment Basis Set Database*, Version 1.0, developed and distributed by the Molecular Science Computing Facility, Environmental and Molecular Sciences Laboratory, Pacific Northwest Laboratory, P. O. Box 999, Richland, WA 99352. Database accessible via the URL http://www.emsl.pnl.gov:2080/forms/basisform.html.
(23) Wadt, W. R.; Hay, P. J. *J. Chem. Phys*. **1985**, *82*, 284.
(24) Glukhovtsev, M. N.; Prossa, A.; Radom, L. *J. Am. Chem. Soc*. **1995**, *117*, 2024.
(25) Gonzalez, C.; Schlegel, H. B. *J. Chem. Phys*. **1989**, *90*, 2154; *J. Phys. Chem*. **1990**, *94*, 5523.
(26) Frisch, M. J.; Trucks, G. W.; Schlegel, H. B.; Scuseria, G. E.; Robb, M. A.; Cheeseman, J. R.; Zakrzewski, V. G.; Montgomery, J. A., Jr.; Stratmann, R. E.; Burant, J. C.; Dapprich, S.; Millam, J. M.; Daniels, A. D.; Kudin, K. N.; Strain, M. C.; Farkas, O.; Tomasi, J.; Barone, V.; Cossi, M.; Cammi, R.; Mennucci, B.; Pomelli, C.; Adamo, C.; Clifford, S.; Ochterski, J.; Petersson, G. A.; Ayala, P. Y.; Cui, Q.; Morokuma, K.; Malick, D. K.; Rabuck, A. D.; Raghavachari, K.; Foresman, J. B.; Cioslowski, J.; Ortiz, J. V.; Stefanov, B. B.; Liu, G.; Liashenko, A.; Piskorz, P.; Komaromi, I.; Gomperts, R.; Martin, R. L.; Fox, D. J.; Keith, T.; Al-Laham, M. A.; Peng, C. Y.; Nanayakkara, A.; Gonzalez, C.; Challacombe, M.; Gill, P. M. W.; Johnson, B.; Chen, W.; Wong, M. W.; Andres, J. L.; Gonzalez, C.; Head-Gordon, M.; Replogle, E. S.; Pople, J. A. *Gaussian 98*, Revision A.9; Gaussian Inc.: Pittsburgh, PA, 1998.
(27) Drougas, E.; Kosmas, A. M. *Can. J. Chem*. **2005**, *83*, 9.
(28) Cotton, A. F.; Wilkinson, G. *Advanced Inorganic Chemistry*, 2nd ed.; Interscience Publishers: New York, 1967.

(29) Lee, T. J.; Dateo, C. E.; Rice, J. E. *Mol. Phys.* **1999**, *96*, 633.
(30) Huie, R. E.; Laszlo, B. In *Halon Replacements. Technology and Science*; Miziolek, A. W., Tsang, W., Eds.; ACS Symposium Series 611; American Chemical Society: Washington, DC, 1995; Chapter 4.
(31) Allan, B. J.; Plane, J. M. C. *J. Phys. Chem. A* **2002**, *106*, 8634.
(32) Drougas, E.; Kosmas, A. M. *Chem. Phys. Lett*. **2004**, *398*, 75.
(33) Bedjanian, Y.; Le Bras, G.; Poulet, G. *J. Phys. Chem. A* **1997**, *101*, 4088.
(34) Bedjanian, Y.; Le Bras, G.; Poulet, G. *J. Phys. Chem. A* **1996**, *100*, 15130.
(35) Chase, M. W. *J. Phys. Chem. Ref. Data* **1996**, *25*, 1297.
(36) Stull, D. R.; Prophet, H. *JANAF Thermochemical Tables*, 2nd ed.; U.S. Government Printing Office: Washington, DC, 1970.